Robust Model Predictive Control of DC-DC Floating Interleaved Boost Converter With Multiple Uncertainties

Hossein Sartipizadeh ⓘ , *Student Member, IEEE*, Farnaz Harirchi ⓘ , *Member, IEEE*, Mohammad Babakmehr ⓘ , *Member, IEEE*, and Payman Dehghanian ⓘ , *Senior Member, IEEE*

Abstract—**DC-DC Floating Interleaved Boost Converter (FIBC) is recently introduced for converting low-level voltage generated by a renewable energy source to high-level voltage required for AC inverters. Although a desired voltage is expected at the output, designing a proper voltage gain for FIBC is challenging due to different types of uncertainties. For instance, the voltage generated by the energy source and, therefore, the input voltage of FIBC may change by a variety of parameters including external load. Furthermore, parametric uncertainty and measurement noise are other sources which can affect the control procedure. As a result, voltage gain for a fixed switching duty cycle may be uncertain. It demands a robust approach to guarantee the control performance under uncertainties without the need for individually tuning controller for each single converter. In this work, a robust model predictive control is employed to regulate the output voltage at the desired level despite the existing uncertainties. Controller parameters are fixed for any FIBC within the uncertainty range and further tuning is not required for individual converters. In addition, unlike the conventional controllers, the suggested controller is able to handle input-output constraints. Performance of the suggested controller is investigated through simulations carried out in MATLAB and the superiority of the proposed approach is verified over non-robust model predictive framework.**

Index Terms—**Approximate convex hull, floating interleaved boost converter, low computational complexity, measurement uncertainty, model uncertainty, robust model predictive control.**

I. INTRODUCTION

RENEWABLE and sustainable energy sources such as photovoltaic (PV) cells commonly produce an unregulated low-level DC voltage. In order to convert the produced power

Hossein Sartipizadeh is with the Institute for Computational Engineering and Sciences (ICES) at the University of Texas at Austin, Austin, TX 78712 USA (e-mail: h.sartipizadeh@gmail.com).

Farnaz Harirchi and Mohammad Babakmehr are with the Electrical and Computer Engineering, Clemson University College of Engineering and Sciences, Clemson, SC 29634-0002 USA (e-mail: harirchi.farnaz@gmail.com; mohammad.babakmehr@gmail.com).

Payman Dehghanian is with the Electrical and Computer Engineering, George Washington University, Washington, DC 20052 USA (e-mail: payman@gwu.edu).

to a proper AC voltage compatible with the grid, a regulated high-level DC voltage is required. A DC voltage in the range of 400 V is desired to feed an AC single-phase 220 V inverter or three-phase 120 V. Although theoretically connecting PV modules in series increases the output voltage, failure of one module causes a disconnection of the whole string and, therefore, this configuration is not reliable. To this end, PV cells are commonly connected in parallel to increase the current, and then a DC-DC boost converter is used to increase the voltage [1]–[5].

Floating Interleaved Boost Converter (FIBC) is a recently developed power electronic interface which has been proposed for low voltage renewable energy resources such as fuel cells and hybrid electric vehicles [6], [7]. This converter consists of two conventional boost converters that are connected in series [1] to increase the obtainable voltage gain while the output voltage ripples are reduced. As a result, FIBC has more components than conventional boost converters. However, it is preferred over conventional converters due to higher efficiency, higher voltage gain, less input ripple, lower voltage and current ratings for switches and diodes, lower switching stress, smaller inductors and capacitors, and lower losses and voltage drop through inductive components [8], [9].

Given a fixed input voltage, the *duty cycle* of boost converter as the design parameter is selected so that the required voltage gain is achieved. Unfortunately, the input voltage of a boost converter varies in practice. For instance in PV cells, although the *Open Circuit Voltage* (VOC) may remain almost constant as long as there is sufficient irradiance light, the output voltage of the PV cell drops when the PV is connected to external loads. This decrement in the voltage of the PV cell is caused by power losses within the cells structure as well as the metallic conductors deposited on the cells surface. Temperature is another factor that also affects the PV cell output voltage. There are different studies on effect of temperature and sun irradiation on PV parameters (for instance see [10]). The output voltage varies about 5% for every 25 °C change in the cell temperature. Therefore, the input voltage of boost converter depends on the sun irradiation condition, temperature, external loads, etc. and consequently, it is uncertain. As a result, choosing the right voltage gain for the boost converter is challenging. In order to compensate any error between the output voltage and its desired, a controller is further used to adjust the converter gain by manipulating the duty cycle.

In literature, control of FIBC has been studied using Proportional-Integral (PI) [1], type III [8], nonlinear adaptive [11], sliding mode [12], [13] and loop shaping [14] controls. Although all of these methods have their own advantages and are reliable in assumed circumstances, they face some major challenges. First, none of these controllers are able to handle input-output constraints. Even for simple cases that input/output are required to be bounded, another device should be used to saturate them which beside requiring another element, it may result in poor performance. Secondly, these controllers are not robust against model uncertainties. It is simply assumed that the model parameters are given (and usually there is no noise associated with the measurements). However practically, manufacturer produces a number of a product which are not necessarily the same and may vary from a unit to another. Physical elements of FIBC, e.g. resistors, capacitors, and inductors, may significantly deviate from their nominal values. Therefore, the system response may differ from its nominal and will be uncertain. Since individually designing and tuning the controller parameters for each unit is not practical, the controller is commonly designed for the nominal parameters with the price of ignoring uncertainty. Authors in [15], [16] investigate the performance of a sliding mode controller in presence of parametric uncertainty and disturbance. An observer is used to potentially account for the bias generated by parameters uncertainty. However, handling input/output constraints using future insights is not applicable to be accounted for in any classic control approach including the sliding mode control.

Nowadays, Model Predictive Control (MPC) is widely adopted in industry as an effective means to deal with nonlinear multi-variable constrained control problems. This type of controller employs an *explicit model* of the plant to predict the system output trajectory in future for the taken actions (inputs). Knowledge of the future is extremely helpful for solving problems on-line and having a better tracking performance in presence of probable disturbances. MPC is also able to handle input-output constraints unlike conventional controllers. Although this approach has been used to control boost converters (for instance see [17]–[19]), and load variations and input voltage disturbances (for a 2-phase converter configuration) have been considered [18], [19], model uncertainty is not taken into account.

In the presence of parametric and measurement uncertainties, for any input sequence, a range of output is expected instead of a single output trajectory. In robust approach, control objectives and physical constraints must be met for all uncertainty realizations or equivalently for the bounds on possible output trajectories. In this case, a single model is not a faithful representation of reality. Therefore, in Robust MPC (RMPC), a set of models called *model set* is employed instead of one model in which the constraints are checked at and satisfied for every model in the model set. Finding a proper model set which captures the uncertainty and provides the bounds on all possible output trajectories may be challenging.

Thus far, different approaches have been suggested for RMPC (see [20]–[27]). Campo and Morari [20] and later Allwright and Papavasiliou [21] utilized the impulse response description to
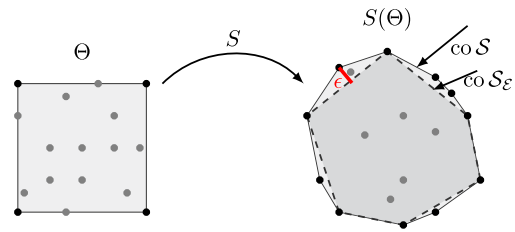

Fig. 1. Mapping the parameters set Θ to the prediction mapping S.

find an appropriate model set and presented their algorithms to solve the robust problem *under conditions that the impulse response is affine in the uncertain parameters*. In this case, control constraints are only required to be checked at the extreme points of parameter box. Unfortunately, the impulse response is rarely affine in the model parameters and this assumption is limiting as this is the case for the FIBC model. In order to tackle this problem, Campi [24], [28] introduced scenario approach. In scenario approach, for any arbitrary system with general dependence of impulse response on parameters, the model set is obtained by randomly sampling the parameter set. However, the number of required samples is still considerably high and many of them are redundant which imposes a high computational complexity for online computation.

A recent work [29]–[31], introduces a new approach to capture the uncertainty for RMPC by reducing the samples of scenario approach and hence reducing the computational complexity of RMPC. This approach that has been proven in fuel cell control in presence of high parametric uncertainty [32], maps the scenario approach sample set Θ to $\mathcal{S} = S(\Theta)$ using a so-called *prediction mapping* S where extreme points of the convex hull of $\mathcal{S}$ provide a bound on all possible output trajectories of Θ and the rest of the samples are redundant and, therefore, can be discarded. It is noted that these models are not necessarily representing the corners of parameter box.

This mapping is illustrated in Fig. 1. Convex hull boundary is drawn with solid line and its extreme points are shown with black dots. Grey points are the redundant elements which can be removed from the model set without any deficiency. In order to further model set reduction, the authors of [31] suggest to use ϵ-approximate convex hull definition in which the number of extreme points are considerably fewer than the convex hull. ϵ-approximate convex hull of set $\mathcal{S}$, shown by $\mathcal{S}_{\mathcal{E}}$, is the best subset of $\mathcal{S}$ so that all points of $\mathcal{S}$ are inside it or not farther than ϵ. The ϵ-approximate convex hull in Fig. 1 is shown with dashed lines and $\mathcal{S}_{\mathcal{E}}$ is the set of its extreme points. Clearly, there is a trade-off between the number of elements of $\mathcal{S}_{\mathcal{E}}$ and approximation error ϵ.

Let t_0 present the current time. Fig. 2 shows all possible output trajectories associated with uncertainty for some single input trajectory in future. The resulted bounds driven by the models of $\mathcal{S}_{\mathcal{E}}$ are shown with dashed lines. Because of the approximation error, the actual output may violate the resulting bounds obtained from $\mathcal{S}_{\mathcal{E}}$. However, authors in [30], [31] separately account for the level of approximation (ϵ) by presenting a dynamic bound on the output violation shown by ϵ_k^y at the future time t_k. As
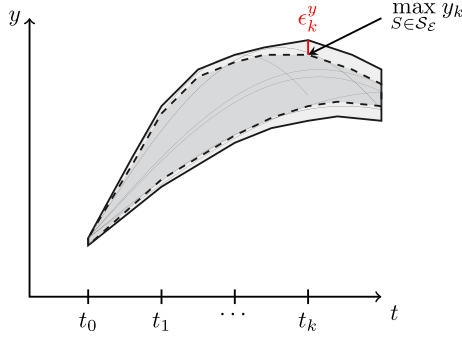
Fig. 2. Output bounds achieved by the approximate convex hull of the prediction mapping S (dashed lines) and after adding the guaranteed output violation bound ϵ^y (solid lines).
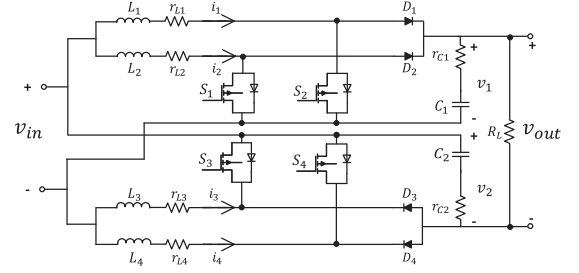

Fig. 3. DC-DC floating interleaved boost converter schematic.

TABLE I
MODEL PARAMETERS

Parameter	Nominal value	Unit	Tolerance
C	2.2 e-3	F	10%
L	1e-4	H	10%
r_C	4.1 e-2	Ω	15%
r_L	2.0 e-2	Ω	15%
R_L	1e3	Ω	20%

a result, one can only check the output constraints at extreme points of ϵ- approximate convex hull while the constraints are adjusted accordingly.

In this paper, we use the new RMPC approach introduced in [31] to regulate the output voltage of a DC-DC floating interleaved boost converter in the presence of:

- *Parametric uncertainty.* Physical elements of system are assumed to be unknown but in a given range.
- *Uncertainty in input voltage.* Input voltage that comes from an energy source is also unknown but in a given range.
- *Measurement uncertainty.* An i.i.d Gaussian noise is assumed on output measures.

We expect to regulate the output voltage at the desired level regardless the existing uncertainties. In fact, we design a unique controller which can perform on every FIBC under the mentioned uncertainties with no need for further tuning. This work is based on the preliminary paper [33] while the violation bounds ϵ^y have been improved in this paper, i.e., a tighter bound is achieved for RMPC which decreases the conservatism of the controller. In addition, the controller performance in a larger uncertainty range as well as in presence of measurement noise is investigated.

This paper is structured as follows: The schematic and model formulation of FIBC converter are discussed in Section II. The formulation of the RMPC used to control the converter is presented in Section III. Section IV explains how to implement this controller to FIBC and the controller performance and its priority against the state of the art is discussed in Section V.

Notation: $\mathbb{R}$ is the set of real numbers, with $\mathbb{R}^n$ a length n vector of real numbers. For $x \in \mathbb{R}^n$, x^T denotes the transpose of x and $[x]_k$ is the kth element of x. It may be represented as x_k when the kth element of x associates with sample time k. For scalar s, $1 \leq s < \infty$, $\|x\|_s := \left(\sum_{i=1}^n |[x]_i|^s\right)^{\frac{1}{s}}$ and $\|x\|_\infty = \max_i |[x]_i|$. Given a set Θ with elements θ and function $f(\theta)$, let $f(\Theta)$ denote the set $\{f(\theta)|\theta \in \Theta\}$. I_r is the $r \times r$ identity matrix. $\mathbf{1}_{n \times m}$ is an n by m matrix of ones. $\mathbf{0}_{n \times m}$ is an n by m matrix of zeros. Given a set $\mathcal{S} \subset \mathbb{R}^n$, $|\mathcal{S}|$ is the number of elements in $\mathcal{S}$, $\text{co} \, \mathcal{S}$ is the convex hull of $\mathcal{S}$. For matrix M let M_r denote the rth row of M. Also for set $\mathcal{S}$ let $\mathcal{S}_r$ be the set of rth row of elements of $\mathcal{S}$. $X \otimes Y$ is the Kronecker tensor product of X and Y.

II. FIBC MODEL

Fig. 3 shows the schematic of an FIBC. It is the connection of two conventional boost converters in series. When the switch S_i is not conducting, corresponding diode, D_i, is closed and when it is conducting, D_i is open. Let D be the FIBC duty cycle and D_0 be its nominal value (refer to [2], [3]) and $\tilde{d}_s$, the duty cycle variation calculated from $\tilde{d}_s = D - D_0$. Then assuming $L_1 = L_2 = L_3 = L_4 = L, C_1 = C_2 = C, r_{L_1} = r_{L_2} = r_{L_3} = r_{L_4} = r_L, r_{C_1} = r_{C_2} = r_C$, the duty cycle to output voltage small signal transfer function of the FIBC converter with resistive load R_L is given below [2], [3]:

$$\frac{\tilde{v}_{out}(s)}{\tilde{d}(s)} = K_v \frac{(1 - (s/\omega_{zr}))(1 + (s/\omega_{zl}))}{(1 + (s/\omega_o Q) + (s^2/\omega_o^2))} \qquad (1)$$

where

$$K_v = \frac{v_{in}\left(2R_L(1-D_0)^2 - r_L(1+D_0)\right)}{(1-D_0)^2\left(R_L(1-D_0)^2 + r_L\right)} \qquad (2\text{a})$$

$$\omega_{zr} = \frac{2R_L(1-D_0)^2 - r_L(1+D_0)}{L(1+D_0)} \qquad (2\text{b})$$

$$\omega_{zl} = \frac{1}{r_C C} \qquad (2\text{c})$$

$$\omega_{zi} = \frac{1}{(R_L C/(D_0+3)) + r_C C} \qquad (2\text{d})$$

$$\omega_o = \frac{1}{\sqrt{LC}}\sqrt{\frac{2R_L(1-D_0)^2 + 2r_L}{R_L + 2r_C}} \qquad (2\text{e})$$

$$Q = \frac{\omega_o(R_L + 2r_C)LC}{R_L C\left(r_L + 2r_C(1-D_0)^2\right) + 2(L + r_C r_L C)} \qquad (2\text{f})$$

FIBC elements can take any number in the given range presented in Table I. v_{in} is uncertain and changes based on the energy source. In order to control the output voltage, $\tilde{d}$ is
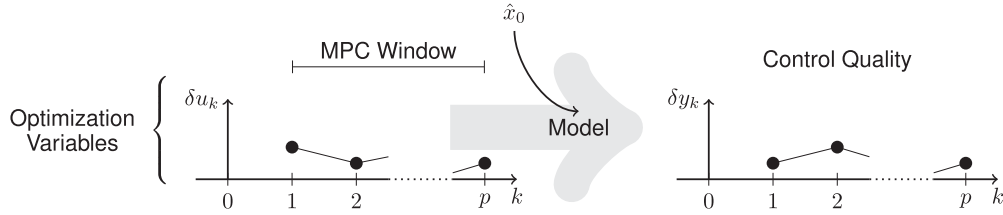
Fig. 4. Model Predictive Control. At each sample time, MPC finds the input sequence that provides the best output behavior of the system over a window of time into the future. The current time is represented by $k = 0$.

manipulated to adjust the absolute duty cycle D. It is noted that although we presented the nominal model with equal indactors and capacitors, we take into account their mismatch by defining the parametric uncertainty in $L, r_L, C,$ and r_C where for instance the uncertainty on L accounts for the accumulative deviation of $L1, L2$ or $L3, L4$ from $2L$. Moreover, the proposed sampling-based controller is compatible with any arbitrary distribution and the given uncertainty in distribution is just an example.

III. RMPC USING AN APPROXIMATE CONVEX HULL

Assume a model of the system is given in the following state space form.

$$x_{k+1} = A(\theta)x_k + B(\theta)\delta u_k$$
$$\delta y_k = C(\theta)x_k. \tag{3}$$

The system to be controlled has m inputs and n outputs with the input at sampling time k represented as $u_k \in \mathbb{R}^m$ and the output as $y_k \in \mathbb{R}^r$. $x \in \mathbb{R}^n$ denotes the vector of system states, $\theta \in \mathbb{R}^q$ is the vector of parameters, and A, B, C are matrices of compatible dimension that are known functions of θ. For time instant k, $\delta u_k := u_k - u_{k-1}$, and $\delta y_k := y_k - y_{k-1}$ are the input output variations. The system parameters lie in the uncertainty set $\Theta_\infty \subset \mathbb{R}^q$. System (3) is assumed to be controllable and observable for all $\theta \in \Theta_\infty$. System output measures at sample time k are denoted by z_k, and it is assumed $z_k = y_k + n_k$, where $n_k \in \mathbb{R}^r$ represents measurement uncertainty.

In basic case when there is no model uncertainty, MPC finds the best feasible future inputs by minimizing an objective function over a p-length prediction horizon subject to input output constraints. A model, which is initiated with its initial state x_0, is used to evaluate the system behavior corresponding to the taken actions. Fig. 4 illustrates the way MPC performs. x_0 can be directly measured or obtained by an estimator (the estimated initial state is indicated by $\hat{x}_0$). In the presence of uncertainty, the robust strategy is to minimize the worst case objective function over all $\theta \in \Theta_\infty$.

Problem 1: Original RMPC problem

$$\min_{u_1,\ldots,u_p} \max_{\theta \in \Theta_\infty} \sum_{k=1}^{p} J(u_k, y_k(\theta))$$

$$x_{k+1} = A(\theta)x_k + B(\theta)\delta u_k, \qquad x_0 = \hat{x}_0$$
$$\delta y_k = C(\theta)x_k, \qquad\qquad k = 1,\ldots,p$$

subject to $u_k = u_0 + \sum_{l=1}^{k} \delta u_l, \; y_k = \hat{y}_0 + \sum_{l=1}^{k} \delta y_l,$

$$y_k^{min} \leq y_k(\theta) \leq y_k^{max},$$
$$Fu_k \leq c. \tag{4}$$

Due to uncertainty in state and output measures, their estimations $(\hat{x}_0, \hat{y}_0)$ are used. Since the original uncertainty set Θ_∞ includes an infinite number of elements, Problem 1 with infinite constraints is intractable. That is why Θ_∞ is replaced by a finite set Θ by taking random samples where the sufficient number of samples can be obtained from the scenario approach (see [24]) for an acceptable violation error and risk of failure. Let $T(\theta)$ be a toeplitz matrix of system impulse response and Σ the summation operator

$$T(\theta) = \begin{bmatrix} h_1(\theta) & 0 & 0 & \cdots & 0 \\ h_2(\theta) & h_1(\theta) & 0 & \cdots & 0 \\ \vdots & & \ddots & \ddots & 0 \\ h_p(\theta) & h_{p-1}(\theta) & \cdots & h_2(\theta) & h_1(\theta) \end{bmatrix}, \tag{5}$$

$$\Sigma = \begin{bmatrix} I_r & & & \\ I_r & I_r & 0 & \\ \vdots & & \ddots & \\ I_r & I_r & \cdots & I_r \end{bmatrix}. \tag{6}$$

Then define two matrices $N(\theta), M(\theta)$ as

$$N(\theta) = \Sigma T(\theta),$$

$$M(\theta) = \left(\mathbf{1}_{p\times 1} \otimes \begin{bmatrix} I_r & \mathbf{0}_{r\times pn} \end{bmatrix} \right.$$
$$\left. + \Sigma \mathcal{O}_p \begin{bmatrix} \mathbf{0}_{n\times r} & I_n & \mathbf{0}_{n\times n(p-1)} \end{bmatrix} \right) \Psi^\dagger(\theta)\Gamma(\theta). \tag{7}$$

Ψ and Γ matrices are defined in (8), and (9) where R and Q are proper weighting matrices to deal with measurement noise. $\Psi^\dagger = (\Psi^T(\theta)\Psi(\theta))^{-1}\Psi^T(\theta)$ is the pseudo inverse of Ψ, and $\mathcal{O}_p$ is the extended observability matrix defined as $\mathcal{O}_p(\theta) = \begin{bmatrix} (CA)^T & (CA^2)^T & \cdots & (CA^p)^T \end{bmatrix}^T$.

$$
\Psi(\theta) =
$$

$$
\begin{bmatrix}
0 & Q^{-\frac{1}{2}} & -Q^{-\frac{1}{2}}A & 0 & \cdots & 0 \\
0 & 0 & Q^{-\frac{1}{2}} & -Q^{-\frac{1}{2}}A & \cdots & 0 \\
\vdots & & \ddots & \ddots & & \vdots \\
0 & 0 & \cdots & 0 & Q^{-\frac{1}{2}} & -Q^{-\frac{1}{2}}A \\
R^{-\frac{1}{2}} & 0 & 0 & \cdots & 0 & 0 \\
R^{-\frac{1}{2}} & -R^{-\frac{1}{2}}C & 0 & \cdots & 0 & 0 \\
\vdots & & \ddots & \ddots & & \\
R^{-\frac{1}{2}} & -R^{-\frac{1}{2}}C & \cdots & -R^{-\frac{1}{2}}C & -R^{-\frac{1}{2}}C & -R^{-\frac{1}{2}}C
\end{bmatrix}
\tag{8}
$$

$$
\Gamma(\theta) =
\begin{bmatrix}
Q^{-\frac{1}{2}}B & & & & & \\
& \ddots & & & 0 & \\
& & Q^{-\frac{1}{2}}B & & & \\
& & & R^{-\frac{1}{2}} & & \\
& & & R^{-\frac{1}{2}} & -R^{-\frac{1}{2}} & \\
& 0 & & \vdots & \vdots & \ddots \\
& & & R^{-\frac{1}{2}} & -R^{-\frac{1}{2}} & \cdots & -R^{-\frac{1}{2}}
\end{bmatrix}
\tag{9}
$$

By integrating a moving horizon estimation (MHE) (using past input-output) for estimating the initial state and output, the predicted output of system (3) in lifted form over a p-length horizon in future can be calculated as [30]

$$
Y_f(\theta) = M(\theta)
\begin{bmatrix}
\Delta U_p \\
z_0 \\
\Delta Z_p
\end{bmatrix}
+ N(\theta)\Delta U_f
\tag{10}
$$

where $Y_f = [y_1^T \cdots y_p^T]^T$ is the future output, $Y_0 = [y_0^T \cdots y_0^T]^T$ is a vector containing repeated elements of the current output, $\Delta U_f = [\delta u_1^T \cdots \delta u_p^T]^T$ is the future input variation vector. $\Delta U_p = [\delta u_{-1}^T \cdots \delta u_{-p+1}^T]^T$, $\Delta Z_p = [\delta z_0^T \cdots \delta z_{-p+1}^T]^T$ are past input and measured output variation vectors, respectively. Define $S(\theta) = \{M(\theta), N(\theta)\}$ as the new mapping and $\mathcal{S} = \{M(\Theta), N(\Theta)\}$ as the set of all possible realizations of uncertainty in the mapping space S. Define $C = \{\alpha \in \mathbb{R}^l \mid \sum_{i=1}^l \alpha_i = 1, \alpha_i \geq 0\}$ and let $\lambda_p, \lambda_f \in \mathbb{R}^p$, where for $k = 1, \ldots, p$,

$$
[\lambda_p]_k(S, \mathcal{S}, s_1) = \min_{\alpha \in C} \left\| M_k - \sum_{i=1}^{|\Theta|} \alpha_i M_k(\theta_i) \right\|_{s_1}
\tag{11a}
$$

$$
[\lambda_f]_k(S, \mathcal{S}, s_1) = \min_{\alpha \in C} \left\| N_k - \sum_{i=1}^{|\Theta|} \alpha_i N_k(\theta_i) \right\|_{s_1}
\tag{11b}
$$

This gives a measure of the error between an arbitrary M and N, and a specific linear combination of the elements of $M(\Theta)$ and $N(\Theta)$. Define the (Hausdorff) distance of an arbitrary S to the convex hull of set $\mathcal{S}$ as

$$
d(S, \mathcal{S}, s_1) = \max\{\|\lambda_p(S, \mathcal{S}, s_1)\|_\infty, \|\lambda_f(S, \mathcal{S}, s_1)\|_\infty\}
\tag{12}
$$

Definition 1: An ϵ-*approximate convex hull* of $\mathcal{S}$ in s_1 distance definition is the convex hull of a minimal subset $\mathcal{S}_\mathcal{E} \subseteq \mathcal{S}$ such that for all $S \in \mathcal{S}$, $d(S, \mathcal{S}_\mathcal{E}, s_1) \leq \epsilon$ [34].

A method introduced in [34] may be used to find $\mathcal{S}_\mathcal{E}$. Let $\mathcal{S}_\mathcal{E} = \{S^{(1)}, \ldots, S^{(E)}\}$ with $S^{(i)} = \{M^{(i)}, N^{(i)}\}$ indicate the set of extreme points of ϵ-approximate convex hull of $\mathcal{S}$. The solution of the following QP problem, with considerably fewer number of constraints and computational complexity is feasible for Problem 1 [31].

Problem 2: RMPC with Approximate Convex Hull

$$
\min_{U_f, t} \quad t
$$

$$
Y_f^{(i)} = M^{(i)}
\begin{bmatrix}
\Delta U_p \\
z_0 \\
\Delta Z_p
\end{bmatrix}
+ N^{(i)}\Delta U_f
$$

$$
\text{subject to } Y_f^{(i)} - \epsilon^y \geq Y^{min} \quad \text{for} \quad i = 1, \ldots, E
\tag{13}
$$

$$
Y_f^{(i)} + \epsilon^y \leq Y^{max}
$$

$$
J(U_f, Y_f^{(i)}) < t
$$

$$
FU_f \leq c
$$

where

$$
\epsilon^y = \epsilon_p \left\| \begin{bmatrix} \Delta U_p \\ \Delta Z_p \end{bmatrix} \right\|_{s_2} + \epsilon_f \|\Delta U_f\|_{s_2}
\tag{14a}
$$

$$
[\epsilon_p]_k = \max_{S \in \mathcal{S}} [\lambda_p]_k(S, \mathcal{S}_\mathcal{E}, s_1) \quad k = 1, \ldots, p
\tag{14b}
$$

$$
[\epsilon_f]_k = \max_{S \in \mathcal{S}} [\lambda_f]_k(S, \mathcal{S}_\mathcal{E}, s_1) \quad k = 1, \ldots, p
\tag{14c}
$$

Remark 1: $\epsilon^y = [\epsilon_1^y, \ldots, \epsilon_p^y]^T \in \mathbb{R}^p$ is a dynamic violation bound on output over the MPC horizon which reflects the approximation error. ϵ^y goes to zero at steady state since the input output variations are zero [30].

Remark 2: $\mathcal{S}_\mathcal{E}$, the approximate convex hull of $\mathcal{S}$ is called *model set*, and its elements are called the *extreme models*.

Remark 3: In this method s_1 and s_2 must be chosen so that $\frac{1}{s_1} + \frac{1}{s_2} = 1$. Therefore, three options $\{s_1 = 1, s_2 = \infty\}$, $\{s_1 = \infty, s_2 = 1\}$, and $\{s_1 = 2, s_2 = 2\}$ can be selected.

In this approach, a trade-off between the time complexity and accuracy is made based on the number of extreme models. Selecting more extreme points increases the number of constraints in (13) and, consequently, increases the computational complexity. However, it results in a smaller ϵ and, therefore, ϵ^y which implies less conservatism. ϵ^y presented in (14a) is less conservative (tighter) than what is used in [33]. Specifically, ϵ_f is also calculated back compared to [33] meaning that the first term associated with the past data is smaller than [33]. The introduced RMPC is briefly implemented as below:

- **Off-line.** Stack the uncertain parameters in vector θ and generate a finite set $\Theta = \{\theta^{(1)}, \ldots, \theta^{(|\Theta|)}\}$ by randomly sampling the uncertainty set. Map Θ to $\mathcal{S} = \{S^{(1)}, \ldots, S^{(|\Theta|)}\}$ where $S^{(i)} = \{M(\theta^{(i)}), N(\theta^{(i)})\}$. For a given ϵ or an allowed number of extreme models, compute $\mathcal{S}_\mathcal{E} = \{S^{(1)}, \ldots, S^{(E)}\} \subset \mathcal{S}$, the best approximate convex hull of $\mathcal{S}$. Calculate $\epsilon_f \in \mathbb{R}^p$ and $\epsilon_p \in \mathbb{R}^p$ using (14).

- **On-line.** Solve (13) at each sample time to find the future input vector U_f. Apply its first element (u_1).

Additional details on the feasibility and stability performance of the proposed model are available in [31].

IV. IMPLEMENTATION

Define the uncertainty vector $\theta = [v_{in}, L, r_L, C, r_C, R_L]^T$. Given the range of each parameter in Table I, we take 1000 random samples with uniform distribution to create the uncertainty set $\Theta = \{\theta^{(1)}, \ldots, \theta^{(1000)}\}$. It is noted that this approach is not limited to uniform distribution; that is for any given distribution (e.g. Gaussian) we only need to draw enough random samples as discussed in [31]. Then we build $\mathcal{S} = \{S(\theta^{(1)}), \ldots, S(\theta^{(1000)})\}$ using the introduced mapping $S(\theta) = \{M(\theta), N(\theta)\}$ with M and N defined in (7) and $Q = R = I$. It is emphasized that if an accurate model is not available, this step can be simply done using the step responses of 1000 random FIBC systems in a lab as our controller only requires the impulse responses. The original RMPC optimization problem to regulate the output voltage at 400 V is

$$\min_{U_f} \max_{\theta \in \Theta_\infty} \quad c_u \|U_f\|_1 + \lambda \|\Delta U_f\| + \gamma \|\zeta\|$$

$$x_{k+1} = A(\theta)x_k + B(\theta)\delta u_k$$
$$\delta y_k = C(\theta)x_k \qquad (15)$$
$$\text{subject to} \quad y_k(\theta) - \zeta_k \leq \mathbf{402} \qquad k = 1, \ldots, p$$
$$y_k(\theta) + \zeta_k \geq \mathbf{400}$$

where A, B, C present the variational system matrices in discrete time state space representation (they are simply obtained from converting (1) to state space form with sampling time $T_s = 1$ ms). $u = \tilde{d}$ is the process input while $y = v_{out}$ and $\delta y = \tilde{v}_{out}$ are the absolute output and its variation. U_f and Y_f are the future input output vectors defined in Section III. c_u is the input cost and the first term of the cost function minimizes the control effort cost. We assume $y_{min} = 400$ V to ensure that the minimum desired output is generated. Since the cost of the input is minimized, this problem turns to a tracking problem. In addition, we set $y_{max} = 402$ V to avoid large peaks in the output at the transient times. However, sometimes there is no feasible solution in the specified output range. To this end, $\zeta = [\zeta_1 \cdots \zeta_p]^T$ is used to soften the output constraints to ensure this problem always has a feasible solution while the potential violation is penalized with γ. $\lambda \|\Delta U_f\|$ attempts to keep the system in the valid range of linearized model and avoid it to go far from the operating point.

Given $\mathcal{S}$ and by setting $s_1 = s_2 = 2$ we calculate its approximate convex hull $\mathcal{S}_\mathcal{E}$ with corresponding $\{\epsilon, \epsilon_p, \epsilon_f\}$ using the method introduced in [34]. According to Problem 2 the following alternative problem can be solved.

$$\min_{U_f} \quad c_u \|U_f\|_1 + \lambda \|\Delta U_f\| + t$$

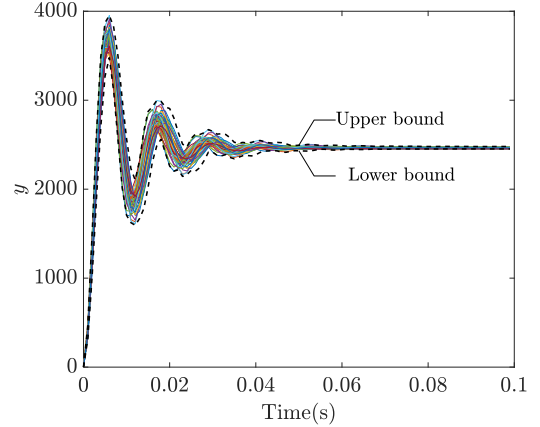$$Y_f^{(i)} = M^{(i)} \begin{bmatrix} \Delta U_p \\ z_0 \\ \Delta Z_p \end{bmatrix} + N^{(i)} \Delta U_f$$

Fig. 5. Step responses of the generated random models for designing the proposed RMPC controller.

$$\text{subject to} \quad Y_f^{(i)} - \zeta + \epsilon^y \leq \mathbf{402} \qquad \text{for} \quad i = 1, \ldots, E$$

$$- Y_f^{(i)} - \zeta + \epsilon^y \leq -\mathbf{400}$$

$$\epsilon^y = \epsilon_p \left\| \begin{matrix} \Delta U_p \\ \Delta Z_p \end{matrix} \right\| + \epsilon_f \|\Delta U_f\|, \gamma \|\zeta\| \leq t \qquad (16)$$

V. SIMULATION RESULTS

The performance of the suggested RMPC against measurement noise, parametric uncertainty and input voltage changes through simulation experiments is investigated in this section. In order to demonstrate the superiority of the proposed approach versus traditional controllers, we compare our RMPC performance to an advanced MPC which is a modified version of existing MPC approaches [17]–[19]; in the sense that an MHE is integrated to enhance their initial state estimation.[1]

A. Experiment Setup and Controller Design

In order to realize the proposed RMPC controller, we generate 1000 random systems in the given uncertainty range as stated in Section IV. Fig. 5 demonstrates the step responses of the generated systems. It is worth noting that the proposed RMPC approach can be applied to any system with a step response that lies between the lower and higher bounds given in Fig. 5. This capability is obtained due to the impulse response integration in the controller formulation (see (5)). It tremendously helps the user to apply the controller without further knowledge about the mathematical model and parameters information in case that only the system step response measure is available.

CVX software is used with solver Sedumi (Gurobi can be used as well) to solve the QP problem (16). We assume that the actual value of FIBC parameters lie in the uncertainty ranges given in Table I. For the experiments, assume the input voltage, received

---

[1]The main superiority of our proposed RMPC controller to non-predictive controllers including PID and sliding mode is its capability to satisfy input-output constraints. In addition, compared to [24], [28] the time complexity of our method is significantly lower as we only use 48 inner models (samples) instead of 500.
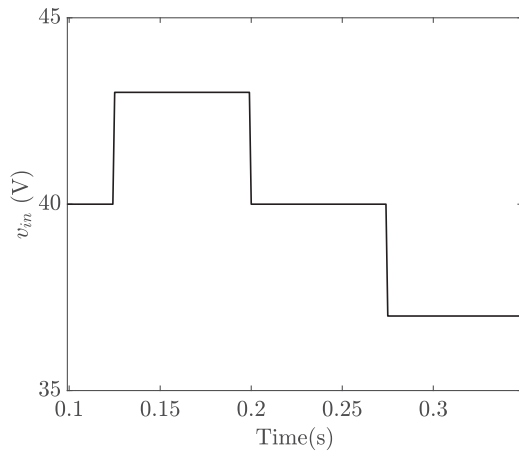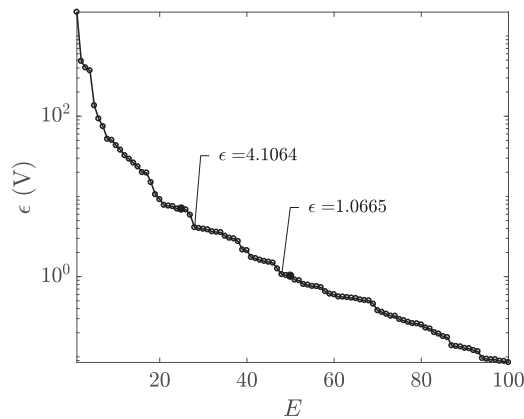
Fig. 6. FIBC input voltage receiving from an energy source.

Fig. 7. Approximation error (ϵ) when uncertainty in mapping S is covered with E elements (extreme models).

Fig. 8. (a) $[\epsilon_p]_k$ (b) $[\epsilon_f]_k$ for $k = 1, \ldots, 10$ when $E = 48$.

Fig. 9. Voltage regulation of 20 random systems using the introduced RMPC under input voltage changes shown in Fig. 6 and parametric uncertainty. (a) Output voltage. (b) Duty cycle deviation from its nominal.

from the energy source, vary over time between 37 V to 43 V as shown in Fig. 6. The control goal is to keep the output voltage at $v_{out} = 400$V for any arbitrary system with parameters within the uncertainty range regardless the unexpected changes in v_{in}. In other words, a unique controller is expected to perform under uncertain situations without any needs for further tuning.

The approximate convex hull computation method presented in [34] was used to find $\mathcal{S}_{\mathcal{E}}$ and results are shown in Fig. 7. The horizontal axis indicates E, the number of elements of $\mathcal{S}_{\mathcal{E}}$, and the vertical axis indicates the resulting ϵ in logarithmic scale. As expected, the approximation error decreases as the number of extreme model increases. According to the figure, choosing 28 extreme models results in $\epsilon = 4.1064$V (about 1% of the steady state output voltage) while picking 48 models decreases the approximation error to 1.0665 V (these points have been highlighted in the figure). Although the user can pick any E, these two points may be good candidates according to the error trend. Since 48 models are still considerably fewer than 1000, in this work we prefer to generate $\mathcal{S}_{\mathcal{E}}$ with 48 elements. As seen, adding more extreme models after $E = 48$ results in a negligible decrement in the approximation error while it still increases the computational complexity.
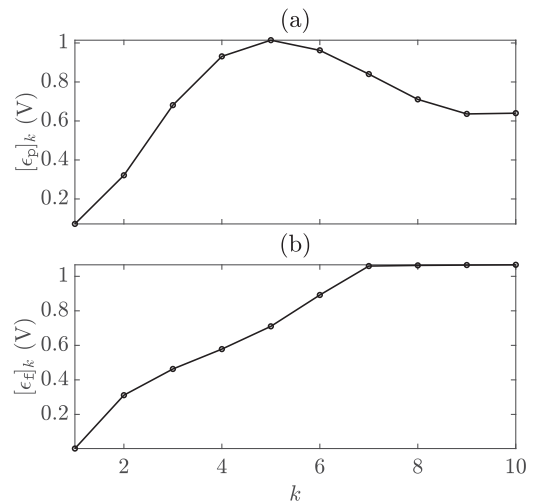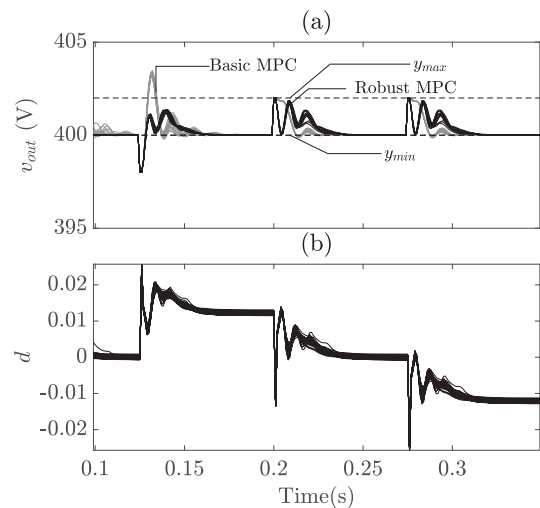
After defining $\mathcal{S}_{\mathcal{E}}$ with 48 elements and $\epsilon = 1.0665$V one may use (14) to calculate back ϵ_p and ϵ_f. Fig. 8 shows ϵ_p and ϵ_f over a 10-length future horizon. As expected, the uncertainty term associated with future times (ϵ_f) expands by time.

Let choose $c_u = 385$, $\lambda = 2500$, and $\gamma = 1.6$ (These weights can change by user based on the importance of their roles stated in Section IV). We initiate the system to reach the steady state, and then apply the robust MPC controller while v_{in} is perturbed as Fig. 6. The controller is tested for 20 arbitrary FIBCs with random parameters in the uncertain ranges.

B. Comparison and Discussion

Fig. 9 compares the tracking results for the random FIBCs controlled by a well-tuned conventional (basic) MPC and the proposed RMPC when there is no measurement noise. Fig. 9(a) shows the output voltage while the necessary changes in the FIBC duty cycle to compensate the disturbance (input voltage perturbation) and parametric uncertainty is presented in

Fig. 9(b). The input-output results are plotted in one figure (Fig. 9) for all the 20 random FIBCs. We individually discuss the performance of the RMPC controller and its privileges vs the basic MPC against the parametric and the input voltage uncertainties. In addition, we investigate output constraint satisfaction as well as the stability performance. It is emphasized that, for the sake of comparison, we have used a highly advance MPC framework which combines an MHE estimator with MPC to remove the DC bias that results in a better performance than a majority of MPCs in the literature.

Controller Performance against input voltage uncertainty. In the case that v_{out} decreases, the RMPC controller adds a small deviation to the duty cycle to cancel out the effect of the input voltage changes. When v_{out} suddenly increases, the controller decreases the duty cycle by adding a negative $\tilde{d}$. The peak is inevitable since it is not predictable. However, the controller tries to return the output trajectory to its desired and also avoids the output to exceed from 402 V. Basic MPC occasionally fails in output constraint satisfaction as it is discussed in bullet c.

Controller Performance against parametric uncertainty. As seen in Fig. 9(a), different systems result in different transient responses. However, the RMPC controller successfully keeps all the system above the desired reference and leads the systems to the desired output at steady state despite the existing uncertainties. Basic MPC, however, might result in instability which is further discussed in bullet d.

Controller Performance in satisfying output constraints. We designated two upper and lower bounds to the output to ensure that the generated voltage always meets the customer desires (400 V) and also do not have unnecessary peaks and overproduction (limited by 402 V). As mentioned, avoiding undesirable peaks caused by sudden disturbances alike input voltage is not possible since we assume that there is no knowledge of their occurrence time. However, except the time at which the voltage goes down by disturbance (and controller brings it back to the accepted region), the output always remains in the expected region despite existing uncertainties. It is worth mentioning that it could not be necessarily achieved by a basic MPC. It is observed that the basic MPC may fail in meeting the constraints as the parameter uncertainty impacts the MPC inner model accuracy and causes a mismatch between the actual system dynamics/DC gain and what the MPC assumes to be the correct one.

Stability. In order to have a fair comparison, the conducted experiments are performed with a one-time controller tuning. The proposed RMPC always maintained the stability in the performed random experiments while basic MPC faced a high fluctuation or even instability in some of the experiments (unstable experiments for basic MPC are removed from Fig. 9(a) for better visualization). It is noted that the individual tuning of basic MPC for every system is either hard and expensive or not practical.

the guaranteed violation bound ϵ^y calculated by the RMPC for $k = 10$ (10-step ahead prediction) is presented in Fig. 10 shows. Fig. 10(a) and Fig. 10(b) represent the violation bounds due to the past input-output and future input (in order, the first and second terms of (14a)), respectively. As claimed in Remark 1, the violation bound goes to zero at steady state, which
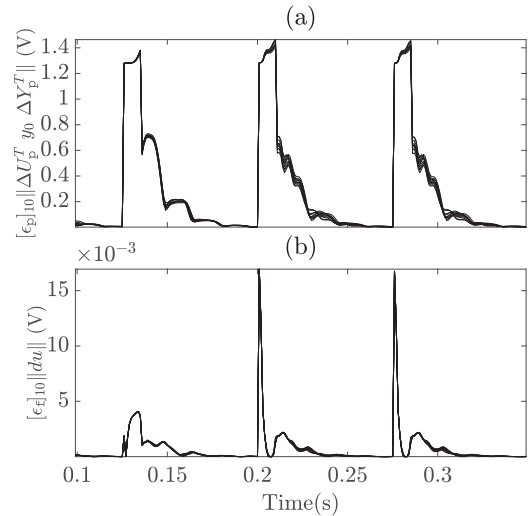

Fig. 10. Output violation bound at future sample $k = 10$ (ϵ^y_{10}) corresponding to the convex hull approximation error (a) due to past input-output variation. (b) due to future input variation.
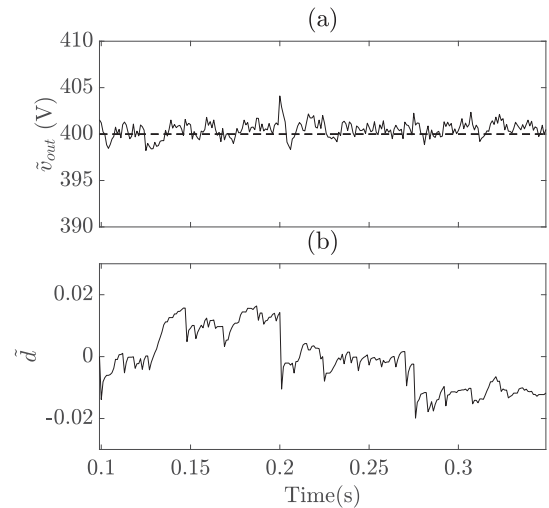

Fig. 11. Voltage regulation of a FIBC (with random θ) by the proposed RMPC under input voltage (as Fig. 6), measurement and parametric uncertainties. (a) Output voltage. (b) Duty cycle deviation from its nominal.

removes the conservatism of the robust approach and results in a bias-free tracking. ϵ^y presented in this work is tighter than that presented in [33]. This tighter bound results in a less conservative controller.

In order to investigate robustness of controller against measurement uncertainty, a Gaussian noise $n_k \sim \mathcal{N}(0, 1\,V)$ is added to the output while the system is selected randomly. Tracking results are shown in Fig. 11 while all types of uncertainties, including input voltage, measurement and parametric uncertainties are involved. Fig. 11 confirms that the controller succeeded in handling multiple uncertainties.

VI. CONCLUSION

In this paper, robust control of an FIBC in the uncertain situations was studied with an attempt to regulate the FIBC output

voltage at the desired level regardless the existing uncertainties. Uncertainty in the FIBC input voltage,in the physical elements (parametric uncertainty), and in the measurement were taken into account as three common types of uncertainty. Specifically, a recent robust model predictive control approach was used due to its capability in handling the parametric uncertainty as well as measurement noise. The key element of this controller compared to the previous robust approaches is its low computational complexity and the given degree of freedom to design it based on the required time complexity. Simulation results confirm the solid and robust performance of the proposed controller under uncertain situations versus an enhanced conventional MPC in the sense of output constraint satisfaction and stability.

References

[1] C. D. Lute, M. G. Simões, D. I. Brandão, A. Al Durra, and S. Muyeen, "Development of a four phase floating interleaved boost converter for photovoltaic systems," in *IEEE Energy Convers. Congr. Expo.*, 2014, pp. 1895–1902.

[2] M. Kabalo, D. Paire, B. Blunier, D. Bouquain, M. G. Simões, and A. Miraoui, "Experimental validation of high-voltage-ratio low-input-current-ripple converters for hybrid fuel cell supercapacitor systems," *IEEE Trans. Veh. Technol.*, vol. 61, no. 8, pp. 3430–3440, Oct. 2012.

[3] M. Kabalo, B. Blunier, D. Bouquain, M. G. Simões, and A. Miraoui, "Modeling and control of 4-phase floating interleaving boost converter," in *Proc. IECON 37th Annu. Conf. IEEE Ind. Electron. Soc.*, 2011, pp. 3026–3032.

[4] M. Babakmehr, F. Harirchi, A. Alsaleem, A. Bubshait, and M. G. Simoes, "Designing an intelligent low power residential PV-based microgrid," in *Proc. IEEE Ind. Appl. Soc. Annu. Meeting*, Oct. 2016, pp. 1–8.

[5] S. Zhuo, A. Gaillard, D. Paire, E. Breaz, and F. Gao, "Design and control of a floating interleaved boost dc-dc converter for fuel cell applications," in *Proc. IECON 44th Annu. Conf. IEEE Ind. Electron. Soc.*, 2018, pp. 2026–2031.

[6] M. Kabalo, B. Blunier, D. Bouquain, M. G. Simôes, and A. Miraoui, "Advanced hybrid dual loop control for multi-phases interleaved floating DC-DC converter for fuel cell applications," in *Proc. IEEE Ind. Appl. Soc. Annu. Meeting*, 2012, pp. 1–8.

[7] S. Choi, V. Agelidis, J. Yang, D. Coutellier, and P. Marabeas, "Analysis, design and experimental results of a floating-output interleaved-input boost-derived DC-DC high-gain transformer-less converter," *IET Power Electron.*, vol. 4, no. 1, pp. 168–180, 2011.

[8] F. Harirchi, M. G. Simões, A. Al Durra, and S. Muyeen, "Short transient recovery of low voltage-grid-tied DC distributed generation," in *Proc. IEEE Energy Convers. Congr. Expo.*, 2015, pp. 1149–1155.

[9] Y. Huangfu, S. Zhuo, F. Chen, and S. Pang, "Evaluation and fault tolerant control of a floating interleaved boost converter for fuel cell systems," in *Proc. Ind. Appl. Soc. Annu. Meeting*, 2016, pp. 1–7.

[10] M. Choobineh, P. C. Tabares-Velasco, and S. Mohagheghi, "Optimal energy management of a distribution network during the course of a heat wave," *Electric Power Syst. Res.*, vol. 130, pp. 230–240, 2016.

[11] H. El Fadil, F. Giri, J. Guerrero, and B. Salhi, "Adaptive control of interleaved boost converter for fuel cell energy," in *Proc. Amer. Control Conf.*, 2011, pp. 3905–3910.

[12] A. Cid-Pastor, R. Giral, J. Calvente, V. Utkin, and L. Martinez-Salamero, "Interleaved converters based on sliding-mode control in a ring configuration," *IEEE Trans. Circuits Syst. I: Regular Papers*, vol. 58, no. 10, pp. 2566–2577, Oct. 2011.

[13] F. Harirchi and H. Sartipizadeh, "Double integral sliding mode control for single-stage active FIBC-PFC in smart grid applications," in *Proc. 9th Annu. IEEE Green Technol. Conf.*, 2017, pp. 7–13.

[14] V. Chapparya, G. M. Krishna, P. Dwivedi, and S. Bose, "Loop shaping controller design for constant output interleaved boost converter using real-time hardware in-the-loop (hil)," in *Proc. Int. Multi Conf. Eng. Comput. Scientists*, 2018, pp. 659–664.

[15] Y. Huangfu, S. Zhuo, F. Chen, S. Pang, D. Zhao, and F. Gao, "Robust voltage control of floating interleaved boost converter for fuel cell systems," *IEEE Trans. Ind. Appl.*, vol. 54, no. 1, pp. 665–674, Jan.-Feb. 2018.

[16] S. Zhuo, A. Gaillard, L. Xu, H. Bai, D. Paire, and F. Gao, "Enhanced robust control of a dc-dc converter for fuel cell application based on high-order extended state observer," *IEEE Trans. Transp. Electrific.*, vol. 6, no. 1, pp. 278–287, Mar. 2020.

[17] M. Aguirre, S. Kouro, J. Rodriguez, and H. Abu-Rub, "Model predictive control of interleaved boost converters for synchronous generator wind energy conversion systems," in *Proc. IEEE Int. Conf. Ind. Technol.*, 2015, pp. 2295–2301.

[18] Y. Liang, Z. Liang, D. Zhao, Y. Huangfu, L. Guo, and B. Zhao, "Model predictive control of interleaved dc-dc boost converter with current compensation," in *Proc. IEEE Int. Conf. Ind. Technol.*, 2019, pp. 1701–1706.

[19] L. Xu, Y. Huangfu, Q. Li, R. Ma, D. Zhao, and Q. Zhang, "Robust control of a interleaved boost converter which feeds a constant power load for electric vehicles," in *Proc. IEEE Transp. Electrific. Conf. Expo.*, 2019, pp. 1–6.

[20] P. J. Campo and M. Morari, "Robust model predictive control," in *Proc. Amer. Control Conf.*, Jun. 1987, pp. 1021–1026.

[21] J. Allwright and G. Papavasiliou, "On linear programming and robust model-predictive control using impulse-responses," *Syst. Control Lett.*, vol. 18, no. 2, pp. 159–164, 1992.

[22] M. V. Kothare, V. Balakrishnan, and M. Morari, "Robust constrained model predictive control using linear matrix inequalities," *Automatica*, vol. 32, no. 10, pp. 1361–1379, 1996.

[23] A. Bemporad, F. Borrelli, and M. Morari, "Min-max control of constrained uncertain discrete-time linear systems," *IEEE Trans. Autom. Control*, vol. 48, no. 9, pp. 1600–1606, Sep. 2003.

[24] M. C. Campi, S. Garatti, and M. Prandini, "The scenario approach for systems and control design," *Annu. Rev. Control*, vol. 33, no. 2, pp. 149–157, 2009.

[25] D. Munoz-Carpintero, M. Cannon, and B. Kouvaritakis, "Recursively feasible robust MPC for linear systems with additive and multiplicative uncertainty using optimized polytopic dynamics," in *Proc. IEEE 52nd Annu. Conf. Decis. Control*, Dec. 2013, pp. 1101–1106.

[26] D. Q. Mayne, "Model predictive control: Recent developments and future promise," *Automatica*, vol. 50, no. 12, pp. 2967–2986, 2014.

[27] T. Campbell and J. How, "Bayesian nonparametric set construction for robust optimization," in *Proc. Amer. Control Conf.*, Jul. 2015, pp. 4216–4221.

[28] G. Calafiore and M. Campi, "The scenario approach to robust control design," *IEEE Trans. Autom. Control*, vol. 51, no. 5, pp. 742–753, May 2006.

[29] H. Sartipizadeh and T. L. Vincent, "Uncertainty characterization for robust MPC using an approximate convex hull method," in *Proc. Amer. Control Conf.*, Jul. 2016, pp. 2699–2704.

[30] H. Sartipizadeh and T. L. Vincent, "Computationally tractable robust moving horizon estimation using an approximate convex hull," in *Proc. 55th IEEE Conf. Decis. Control*, 2016, pp. 3757–3762.

[31] H. Sartipizadeh and T. L. Vincent, "A new robust MPC using an approximate convex hull," *Automatica*, vol. 92, pp. 99 115–122, Jun. 2018.

[32] H. Sartipizadeh and T. L. Vincent, "Robust model predictive control of a catalytic autothermal methane reformer for fuel cell applications," *Control Eng. Pract.*, vol. 76, pp. 31–40, 2018.

[33] H. Sartipizadeh and F. Harirchi, "Robust model predictive control of DC-DC floating interleaved boost converter under uncertainty," in *Proc. 9th Annu. IEEE Green Technol. Conf.*, 2017, pp. 320–327.

[34] H. Sartipizadeh and T. L. Vincent, "Computing the approximate convex hull in high dimensions," 2016, *arXiv:1603.04422*.

Hossein Sartipizadeh (Student Member, IEEE) received the B.S. degree in electrical engineering control systems from the Iran University of Science and Technology, Tehran, Iran, in 2009, the M.S. degree in electrical engineering control systems from the Sharif University of Technology, Tehran, in 2011, and the Ph.D. degree in electrical engineering control systems & signal info from the Colorado School of Mines, Golden, CO, USA, in 2017. He was a Postdoctoral Fellow with the University of Texas at Austin, Austin, TX, USA, and a Visiting Scientist with the William E. Boeing Department of Aeronautics & Astronautics, University of Washington, Seattle, WA, USA (2017–2018). He is currently with Ford Motor Company. His research interests include uncertainty characterization, robust model predictive control under deterministic/stochastic uncertainties, and data selection in high dimensions.

Farnaz Harirchi (Member, IEEE) received the B.S. degree in electrical engineering from Central Tehran University, Tehran, Iran, in 2008, the M.Sc. degree in electrical and electronic engineering from the Iran University of Science and Technology, Tehran, Iran, in 2011, and the Ph.D. degree in electrical engineering with specialties in power electronics from the Department of Electrical Engineering and Computer Science, Colorado School of Mines, Golden, CO, USA, in December 2017. She was a Postdoctoral Associate with Clemson University in Charleston, North Charleston, SC, USA. She is currently a Project Engineer with S&C electric company, Chicago, IL, USA. Her research interests include renewable energy aggregation, smart microgrids, power electronics, protection systems, and intelligent control for high-power electronics applications.

Payman Dehghanian (Senior Member, IEEE) received the B.Sc. degree in electrical engineering from the University of Tehran, Tehran, Iran, in 2009, the M.Sc. degree in electrical engineering from the Sharif University of Technology, Tehran, Iran, in 2011, and the Ph.D. degree in electrical engineering from Texas A&M University, College Station, TX, USA, in 2017. He is currently an Assistant Professor with the Department of Electrical and Computer Engineering, George Washington University, Washington, D.C., USA. His research interests include power system reliability and resiliency, power system protection and control, asset management, and smart electricity grid applications. He was the recipient of the 2013 IEEE Iran Section Best M.Sc. Thesis Award in electrical engineering, the 2014 and 2015 IEEE Region 5 Outstanding Professional Achievement Awards, and the 2015 IEEE-HKN Outstanding Young Professional Award.

Mohammad Babakmehr (Member, IEEE) received the B.S. degree in electrical engineering from Central Tehran University, Tehran, Iran, in 2008, the M.Sc. degree in biomedical-bioelectric engineering from the Amirkabir University of Technology, Tehran, Iran, in 2011, and the M.Sc. and Ph.D. degrees in electrical engineering from the Colorado School of Mines, Golden, CO, USA, in 2016 and 2017, respectively. He was a Research Associate with Clemson University in Charleston, North Charleston, SC, USA. He is currently a Senior Data Scientist with Ford Motor company. His research interests include artificial intelligence, machine learning, smart grid technologies, signal processing, and big data analytics.